DYNAMIC SITE CHARACTERIZATION OF CHRISTCHURCH STRONG MOTION STATIONS

Clinton M. Wood[1], Brady R. Cox[2], Liam M. Wotherspoon[3], and Russell A. Green[4]

SUMMARY

This paper details efforts to characterize the small-strain dynamic properties of 13 strong motion station (SMS) sites in the greater Christchurch, New Zealand area. These SMS recorded a unique set of ground motions (GM) from the 2010-2011 Canterbury earthquakes. Currently, little information about the subsurface layering and dynamic characteristics at these 13 SMS is available. Information provided by GeoNet consists only of generalised layering based on regional geological characteristics and nearby well logs, with no information on dynamic properties. Consequently, the seismic site classifications of these sites were largely based on assumptions. To better define the site classifications, we performed active- and passive-source surface wave testing to obtain shear wave velocity (Vs) profiles at each site. The Vs profiles were used to calculate the average Vs over the top 30 m of the subsurface and to estimate the natural period of vibration (Tn). Additionally, estimates of Tn were obtained by computing the horizontal-to-vertical spectral ratios from recorded GM at each SMS. Based on this new information, we have updated the site classifications at the 13 SMS sites tested; 10 of which ended up with a slightly different site classification than the original assumption (often one site class lower).

INTRODUCTION

The Christchurch, New Zealand region has been significantly impacted by a sequence of earthquakes that began on 4 September 2010 with the moment magnitude (M_w) 7.1 Darfield earthquake, which was located approximately 37 km to the west of central Christchurch [1]. In the year following this event, 28 earthquakes occurred within 40 km of the city that had local magnitudes (M_L) greater than 5.0 [2]. Figure 1 shows the epicentres of nine of the more significant events in this sequence; the most devastating of which was the 22 February 2011, M_w6.2 Christchurch earthquake that occurred beneath the south eastern edge of the city at 12:51 pm local time, 22 February 2011. The close proximity, shallow depth, and fault mechanism from this event resulted in ground motions (GM) in the city that were considerably larger than those during the Darfield earthquake. At many locations, the seismic demands placed on the built environment were higher than engineering design levels (500- and 2,500-yr return period), resulting in structural damage and collapse, especially within the central business district (CBD) of Christchurch. This earthquake resulted in 181 casualties, thousands of injuries, and widespread soil liquefaction that caused billions of dollars of damage to buildings, homes and infrastructure.

The GM from these devastating earthquakes were recorded by a network of strong ground motion recording stations (often simply referred to as strong motion stations – SMS) in the greater Christchurch area. These SMS are part of both the National Strong Motion Network (NSMN) and the Canterbury Accelerograph Network (CanNet) [3] and fall under the auspices of the GeoNet project (http://www.geonet.org.nz). They captured an extensive and unique set of ground motion records during the Canterbury earthquake sequence. However, at present, there is little information available on the subsurface site characteristics at these SMS, with layering profiles and seismic site classes assumed from regional geological knowledge and nearby well logs. To fully understand the variability of ground shaking across the region, and the effects of local site conditions on the amplitude, frequency content, and duration of shaking, dynamic site characterization is needed to define the properties of the subsurface at each SMS.

This paper details efforts to characterize the small-strain dynamic properties at 13 of the 19 strong motion stations in Christchurch, Lyttelton, and Kaiapoi. The 13 stations where dynamic testing was performed are shown in Figure 1. Additional information about these stations is presented in Table 1. Both active- and passive-source surface wave testing were used to determine the shear wave velocity (Vs) profiles at the indicated SMS. Active-source methods included a combination of the Spectral Analysis of Surface Waves (SASW) [4,5] and the Multi-channel Analysis of Surface Waves (MASW) [6], while passive-source methods included a combination of linear [7,8] and 2D microtremor array methods (MAM) [9,10].

The Vs profiles derived from surface wave testing were used to calculate the average Vs over the top 30 m of the subsurface (i.e., Vs30 values) and to estimate the natural period of

[1] *Ph.D. Candidate, University of Arkansas, Fayetteville, AR, USA*

[2] *Assistant Professor, University of Arkansas, Fayetteville, AR, USA*

[3] *EQC Research Fellow, University of Auckland, Auckland (member)*

[4] *Associate Professor, Virginia Tech, Blacksburg, VA, USA*

vibration (Tn) at each SMS. Additional estimates of Tn were obtained by computing the horizontal-to-vertical spectral ratios (H/V) from recorded GM at each SMS. Based on this new information, we have updated the site classifications at the 13 SMS sites tested.

BACKGROUND

The city of Christchurch is located on the central coast of the Canterbury Plains on the South Island of New Zealand; a region 50-km wide and 160-km long formed by overlapping alluvial fans deposited by eastward flowing rivers from the Southern Alps mountain range into Pegasus Bay. The majority of the city is located on Canterbury Plains Holocene deposits, although the southern edge of the city is on the weathered basalt and thick Pleistocene loess deposits of the Port Hills [11]. Much of Christchurch was originally swampland, beach dune sand, estuaries, lagoons, river channel and flood plain deposits, which were drained as part of the European settlement and expansion of the city [12]. The surface geology is comprised of the Springston formation: fluvial gravels, sands and silts up to 20 m in thickness; and the Christchurch formation: estuarine, lagoon, dune, and coastal swamp deposits of gravel, sand, silt, clay and peat up to 40 m thick. The nature of this depositional environment means that there can be significant variations in the characteristics of the shallow soil over small distances. These near surface sediments overlie 300- to 400-m of late Pleistocene sands and gravels [11]. Similar geologic conditions exist in Kaiapoi, a town 17 km north of Christchurch on the Canterbury Plains, in an area where extensive natural and manmade river channel modifications have occurred since European settlement [13].

Strong Motion Stations

Prior to 2006, there were only seven SMS in the Christchurch area. These stations were part of the NSMN and operated under the auspices of the GeoNet project, an integrated geological hazard monitoring system. Given the variability of the fluvial and estuarine surface geology within the city, this limited number of sites was deemed insufficient to record expected variations in GM characteristics over short distances due to local site effects in future earthquakes. As such, CanNet was developed to increase the number of SMS in the region.

CanNet is a network of low cost, low maintenance accelerographs in the Canterbury region developed at the University of Canterbury [3]. Currently, 37 additional CanNet SMS have been installed, and when fully implemented, the CanNet project will enhance the coverage of the existing NSMN stations in the Canterbury region with 60 SMS. The system was originally proposed to record the anticipated motions from earthquakes occurring on the Alpine Fault and Marlborough fault system. However, instead, the instruments captured a large dataset of strong motion records from the 2010-2011 earthquake sequence. Ten CanNet SMS and seven NSMN SMS in Christchurch and Lyttelton, and one CanNet SMS located in Kaiapoi recorded the earthquakes. Following the major earthquakes, in August 2011 an additional SMS was installed in the suburb of Halswell as part of the NSMN. Both the NSMN SMS and the CanNet SMS are currently operated as part of the GeoNet project, with 19 total permanent SMS in the greater Christchurch area and Kaiapoi.

Table 1: Supplemental information for strong motion stations (SMS) in, and around, Christchurch, New Zealand

Station Code*	Station Name	Latitude**	Longitude**	Assumed Seismic Site Class***	Surficial Geology****
CACS	Canterbury Aero Club	-43.48317	172.53001	D	Gravel
CBGS	Christchurch Botanical Gardens	-43.52934	172.61988	D	Alluvial sand and silt with gravels > 3 m
CCCC	Christchurch Cathedral College	-43.53809	172.64743	D	Alluvial sand and silt with gravels > 3 m
CHHC	Christchurch Hospital	-43.53593	172.62752	D	Alluvial sand and silt
CMHS	Christchurch Cashmere High School	-43.56562	172.62417	D	Alluvial sand and silt with gravels > 3m
CRLZ	Canterbury Ring Laser	-43.57474	172.62322	B (Cavern)	Rock
HALS	Halswell School	-43.50686	172.73135	U	Alluvial sand and silt
HPSC	Hulverstone Drive Pumping Station	-43.50157	172.70219	E	Dune and beach sand
HVSC	Heathcote Valley Primary School	-43.57978	172.70942	C	Loess-volcanic derived colluvium
KPOC	Kaiapoi North School	-43.37646	172.66376	E	Alluvial sand and silt
LPCC	Lyttelton Port Company	-43.60784	172.72477	B	NA
NBLC	New Brighton Library	-43.50686	173.73135	U	Dune and beach sand
NNBS	North New Brighton School	-43.49542	172.71800	E	Dune and beach sand
PPHS	Papanui High School	-43.49284	172.60691	D	Alluvial sand and silt with gravels > 3m
PRPC	Pages Road Pumping Station	-43.52580	172.68276	E	Alluvial sand and silt
REHS	Christchurch Resthaven	-43.52195	172.63515	D	Peat swamp & unconsolidated sand with gravels > 3 m
RHSC	Riccarton High School	-43.53617	172.56440	D	Alluvial sand and silt with gravels > 3m
SHLC	Shirley Library	-43.50533	172.66339	D-E	Alluvial sand and silt with gravels > 3m
SMTC	Styx Mill Transfer Station	-43.46753	172.61386	D-E	Alluvial sand and silt

* Note that dynamic characterization of Christchurch strong motion stations CACS, CRLZ, HALS, NBLS, PPHS and SMTC was not performed in this study

** Latitude and longitude provided in WGS84 coordinate system

*** Seismic site class (according to NZS1170.5) assumed by GeoNet based on nearby well logs and geology or obtained from Cousins and McVerry (2010). U stands for unknown.

**** Surficial geology from Brown and Weeber 1992.

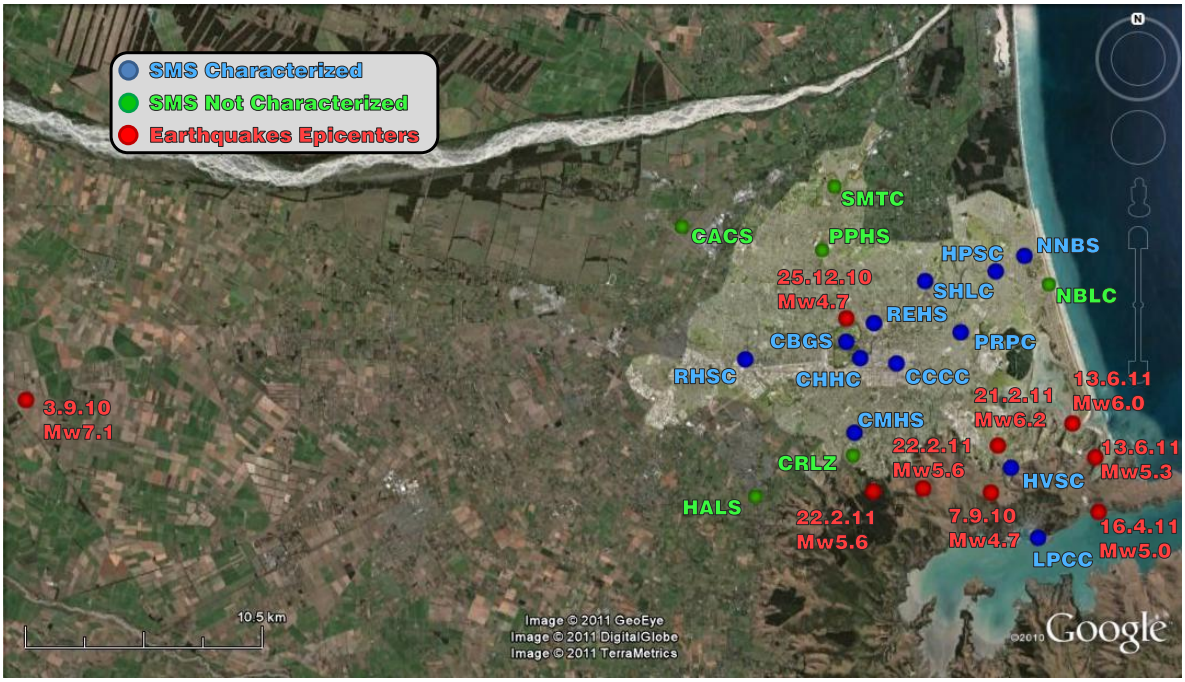

Figure 1: ***Locations of strong motion stations (SMS) in, and around, Christchurch, New Zealand. Blue symbols indicate SMS where dynamic site characterization was performed (note KPOC not shown). Also shown are the epicentral locations of nine of the more significant earthquakes in the 2010-2011 sequence.***

Currently, little information is available from GeoNet on the geotechnical site characteristics at the SMS in Christchurch, other than some generalised subsurface layering based on regional geological characteristics and nearby well logs [2]. No information is available on the small-strain dynamic properties for the SMS sites, which are important for understanding the potential for amplification of ground shaking. Local site characteristics have a significant influence on surface ground motions, and are currently accounted for in code-based design using the A/B/C/D/E seismic site classification system [14]. The assumed site classes of the SMS investigated in this study are summarised in Table 1, using information from GeoNet, and Cousins and McVerry [15]. Eight of the SMS in the region of interest are currently defined as Site Class D, due to the deep gravel layers that overlie bedrock beneath much of Christchurch. Four SMS are defined as Site Class E, controlled by the assumed existence of greater than 10 m of very low strength material (undrained shear strength s_u < 12.5 kPa, SPT N < 6, or Vs < 150 m/s) [14], and two are on the borderline of Site Class D and E (D-E). Often, the surficial geology of the sites that are defined as Site Class D or E (refer to Table 1) is similar; making it difficult to assign detailed site classifications based on geology alone, Only three stations are assumed to be located on more competent material; LPCC and CRLZ on Site Class B (Rock), and HVSC on Site Class C (Shallow Soil). Finally, two of the SMS had no site subsoil class definition (U = unknown).

Ground Motions

The energy magnitude (M_e) of the Darfield earthquake is relatively high compared to its moment magnitude (M_w) (i.e., M_e8.0 versus M_w7.1). This relatively large energy release, combined with rupture directivity effects, resulted in larger ground motions in Christchurch than would have been predicted prior to the event [15]. Site, topographic, and basin effects may have further influenced the ground shaking at the SMS across Christchurch. The maximum horizontal peak ground acceleration (PGA) recorded in the Christchurch CBD during the Darfield earthquake was 0.25g (geometric mean of the horizontal components) at the REHS SMS. The largest recorded horizontal PGA in greater Christchurch was 0.61g at the HVSC SMS, located at the head of the Heathcote Valley. HVSC also experienced very high spectral accelerations in the short-period range, likely a result of basin wedge effects [16]. The spectral accelerations of the Darfield earthquake GM were generally less than the 500-year design spectrum for the Christchurch region. However, the effect of thick soil layers over rock was evident in the motions from select SMS (e.g., CCCC and CHHC). The response spectra at these stations had peaks at a period of approximately 2.5 seconds, which is likely a result of the long period energy of the earthquake and the natural site period. For more information on the geotechnical effects of the Darfield earthquake refer to Allen *et al.* [17,18].

The motions from the Christchurch earthquake were, in many places, more intense than those from the Darfield event. This was primarily because the rupture plane for the Christchurch earthquake was beneath the south eastern edge of the city. Horizontal PGAs of between 0.37g and 0.52g were experienced in the CBD during the Christchurch earthquake. The largest recorded motions were near the epicentre at HVSC, with horizontal and vertical PGAs of 1.41g and 2.21g, respectively [16]. Response spectral accelerations of the recorded ground motions were higher than the 500-year design spectrum over the entire range of engineering interest. Similar to the Darfield earthquake motions, peaks in the response spectra of several CBD stations (e.g., CBGS, CCCC, CHHC and REHS) were pronounced at long periods, (0.4 – 2.0 s), exceeding the 2,500-year design levels in this region.

As with the Darfield earthquake, the M_e of the Christchurch earthquake is relatively high compared to its M_w (i.e., M_e6.75 versus M_w6.2). Again, site, topographic and basin effects likely further influenced the ground motions throughout the city. Fry et al. [19] indicate that not all features of the strong motion records can be explained by source effects, and highlights the need for detailed analysis of the shallow subsurface.

SHEAR WAVE VELOCITY PROFILING

Surface wave testing was performed at 13 SMS in the greater Christchurch area on 3-12 August 2011 (refer to Figure 1 and Table 1). The surface wave testing was conducted as close to the actual SMS as practical (typically within 10-50 m). However, in the case of LPCC, the testing location was approximately 300 m from the SMS due to limited access to the port area. At each test site, a combination of active-source (SASW and MASW) and passive-source (1D and 2D MAM) surface wave techniques were used to resolve the shear stiffness and layering beneath each station. Linear array (1D) testing employed a receiver array composed of 24, 4.5-Hz geophones with an equal spacing (dx) of approximately 1.5-m (a total array length of 35 m). For REHS, a 0.9 m receiver spacing was used due to limited space around the site. An L-shaped array with receivers placed at 1.5 m intervals was also used for 2D MAM measurements at all SMS. For active-source testing, a 5.4 kg sledgehammer was used to generate surface wave energy.

At sites with surface soil conditions, a P-wave refraction survey was performed using the linear array (P-wave refraction could not be conducted at sites with asphalt or concrete at the surface). These measurements were used to determine the depth to saturation (ground water table) at each station for input into the surface wave inversion and future liquefaction analyses. For refraction testing, five hammer blows (shots) located one receiver spacing in front of the first receiver were stacked to increase the signal-to-noise ratio. At this same source location, SASW data was also collected using select pairs of geophones within the linear array. Typical receiver spacing's included 1dx, 2dx, 3dx, 4dx, 6dx, 8dx, 10dx and 12dx. These pairs of receivers were always chosen to maintain the source-to-first receiver distance equal to the first-to-second receiver distance, as is typical in SASW testing [5]. Following the SASW data collection, MASW testing was performed using three separate source locations of 4.6 m, 9.1 m and 18.3 m from the first receiver in the array; resulting in array-centre distances of 22.1 m, 26.6 m, and 35.8 m [20]. As with the P-wave refraction, at least five sledgehammer blows were average together at each source location during surface wave testing to increase the signal-to-noise ratio.

Linear array passive surface wave testing (i.e., ReMi as described in Louie [7]) was conducted using the same array used for active testing. During passive testing, a total of 10, 32-s long noise signals were recorded. Then, the linear array was converted into a 2D array by rotating 12 of the 24 geophones 90 degrees; resulting in a 16.7 m x 18.2 m L-shaped array. The 2D passive array has several advantages over a linear passive array, the most important of which is the ability to resolve the direction of surface wave propagation. The lack of directional information when using a linear passive array can lead to significant errors in velocity profiles under certain circumstances and caution should be exercised when using this method without other corroborating active or 2D passive methods [21].

The SASW data was analysed using the phase unwrapping method to determine the individual dispersion curves from each receiver spacing. The individual dispersion curves were then combined to form a composite dispersion curve over the frequencies/wavelengths of interest. The MASW data was analysed using the frequency domain beamformer method [22]. For each source offset, a dispersion curve was generated by picking the maximum spectral peak in the frequency/wavenumber domain. The linear array passive data was analysed using the two-dimensional slowness-frequency (p-f) transform in the software SeisOpt ReMi [23]. The 2D MAM data was analysed using the 2D frequency domain beamformer method [22]. Further information about the general surface wave processing methods can be found in Cox and Wood [24].

Once the surface wave dispersion trends from each method were obtained, a mixed-method composite dispersion curve was generated by combining the dispersion data from each active and passive surface wave method. The dispersion data was then divided into 30 wavelength bins using a log distribution. The mean phase velocity and associated standard deviation was then calculated for each bin, resulting in an experimental dispersion curve with associated uncertainty (Figure 2a). The shear wave velocity profile was then determined by fitting a 3D theoretical solution to the mean experimental dispersion curve using the software WinSASW (Figures 2a and 2b). The 3D solution uses the superposed-

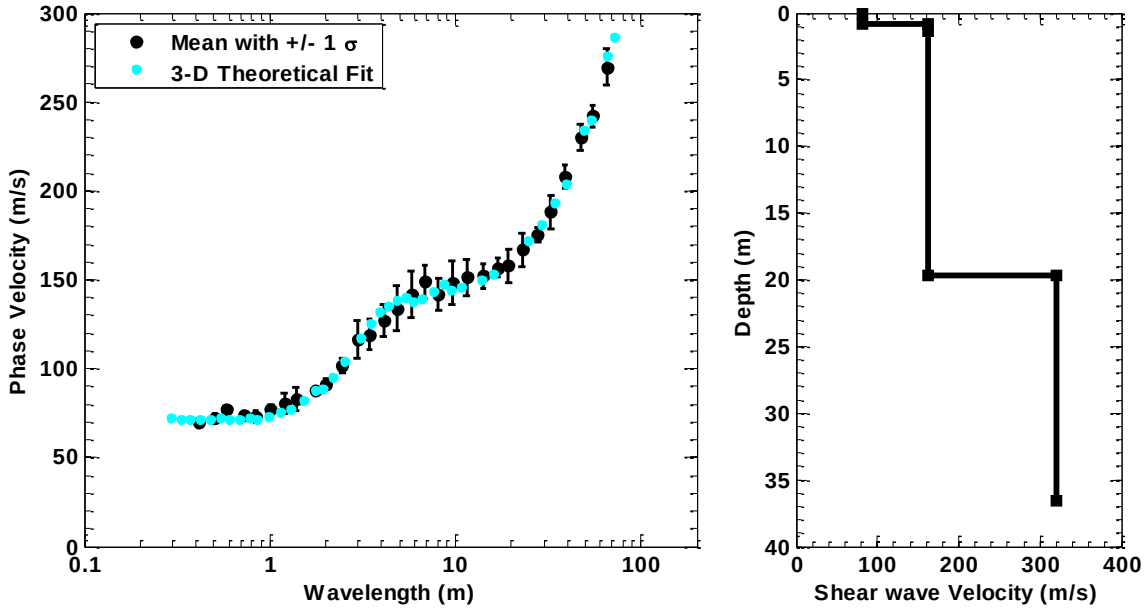

(a) (b)

Figure 2: Dispersion curve (a) and shear wave velocity profile; (b) for SMS CBGS.

Table 2: Shear wave velocity profiles for SMS tested in, and around, Christchurch, New Zealand

CBGS		CCCC		CHHC		CMHS		HPSC		HVSC		KPOC	
Depth (m)	Vs (m/s)	Depth (m)	Vs (m/s)	Depth (m)	Vs (m/s)	Depth (m)	Vs (m/s)	Depth (m)	Vs (m/s)	Depth (m)	Vs (m/s)	Depth (m)	Vs (m/s)
0.0	80	0.0	320	0.0	380	0.0	100	0.0	90	0.0	340	0.0	150
0.9	80	0.2	320	0.1	380	1.2	100	0.6	90	0.1	340	0.3	150
0.9	160	0.2	140	0.1	120	1.2	130	0.6	110	0.1	150	0.3	110
19.6	160	17.6	140	2.1	120	4.2	130	7.8	110	1.2	150	1.5	110
19.6	320	17.6	460	2.1	180	4.2	180	7.8	240	1.2	270	1.5	150
36.6	320	61.0	460	24.1	180	22.5	180	18.4	240	4.4	270	8.2	150
				24.1	370	22.5	760	18.4	400	4.4	370	8.2	270
				36.6	370	61.0	760	33.5	400	17.5	370	17.4	270
										17.5	760	17.4	490
										48.8	760	61.0	490

LPCC		NNBS		PRPC		REHS		RHSC		SHLC	
Depth (m)	Vs (m/s)	Depth (m)	Vs (m/s)	Depth (m)	Vs (m/s)	Depth (m)	Vs (m/s)	Depth (m)	Vs (m/s)	Depth (m)	Vs (m/s)
0.0	300	0.0	240	0.0	120	0.0	120	0.0	140	0.0	200
0.3	300	0.1	240	0.7	120	0.3	120	0.5	140	0.6	200
0.3	150	0.1	110	0.7	200	0.3	100	0.5	180	0.6	120
0.9	150	1.3	110	2.0	200	6.1	100	10.8	180	6.1	120
0.9	270	1.3	130	2.0	160	6.1	90	10.8	460	6.1	210
3.4	270	12.0	130	15.8	160	13.7	90	48.8	460	21.3	210
3.4	370	12.0	370	15.8	300	13.7	240			21.3	370
6.4	370	36.6	370	33.5	300	30.5	240			39.6	370
6.4	1520										
61.0	1520										

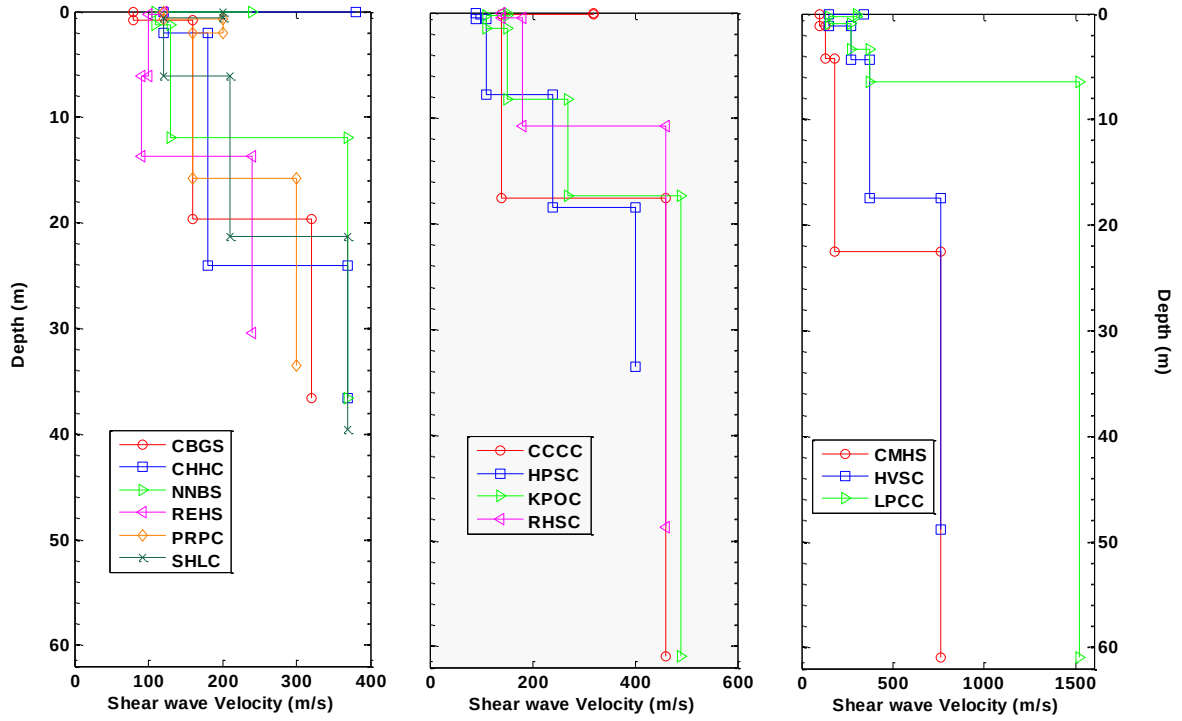

Figure 3: Vs profiles with (a) V_{smax} < 400 m/s; (b) Vs profiles with 400 <V_{smax}< 600 and (c) Vs profiles with V_{smax}> 600 m/s.

mode dynamic stiffness matrix method to solve for the surface displacements generated by all Rayleigh wave modes and body waves [25]. The solution is the most appropriate solution for SASW and can also be used to account for the smearing/superposition of modes that can exist in MASW dispersion data at longer wavelengths due to a lack of spatial resolution. The shear wave velocity profiles obtained from the inversions for each site were limited to the maximum experimental wavelength divided by two (i.e., λmax/2).

The shear wave velocity profiles for each SMS are presented in Table 2 and plotted in Figure 3. All profiles extend to at least 30 m below the surface, while some extend as deep as 60 m. In Figure 3, the Vs profiles have been grouped according to the maximum velocity encountered (V_{Smax}). Figure 3a is for profiles with V_{Smax} < 400 m/s, Figure 3b is for profiles with 400 m/s < V_{Smax} < 600 m/s, and Figure 3c is for profiles with V_{Smax} > 600 m/s. From these figures, it is obvious that greater profiling depths were possible at stiffer sites (i.e., sites with greater V_{Smax} values). As expected, the majority of the profiles (10 of 13) have a soft soil layer (Vs < 200 m/s) ranging from 6- to 20-m thick near the surface (refer to Figures 3a and 3b). Of these sites, REHS, NNBS, CBGS and CCCC have the thickest and/or softest soil layers, which are in excess of 10-m thick with Vs of 160 m/s or less. At REHS in particular, the average velocity over the top 13.5 m is

less than 100 m/s. REHS is the only SMS located on surficial geology classified as peat (refer to Table 1). Rock (Vs > 760 m/s) was encountered at only three of the SMS tested (CMHS, HVSC and LPCC; refer to Figure 3c), all of which are within close proximity to the Port Hills, where rock is expected at shallower depths (refer to Figure 1). The Vs30 values calculated from the Vs profiles at each SMS are provided in Table 3. These values are discussed in more depth in the Seismic Site Classification section.

SITE PERIOD ESTIMATES

The small strain, fundamental periods of the SMS sites were estimated using three approaches. The first and most simple approach assumed that the site profile is linear elastic, which is reasonable for small strain conditions. The average shear wave velocity for the profile (V_{Savg}) down to the top of bedrock, or to the maximum depth that Vs was characterized when bedrock was not encountered, was determined by equating the time that it takes a wave to propagate from the base of the profile to the ground surface in the measured (layered) profile and in an "equivalent uniform profile." The equivalent uniform profile has the same overall thickness as the measured profile, but consists of a single layer having the shear wave velocity V_{Savg}. By equating the travel times for the two profiles, V_{Savg} is determined as:

$$V_{S\,avg} = \frac{\sum_i h_i}{\sum_i \frac{h_i}{V_{Si}}} \qquad (1)$$

where: h_i is the thickness of layer i and V_{Si} is the small strain shear wave velocity of layer i. The characteristic, or fundamental, period (Tn) of the equivalent uniform profile is determined by (e.g., Kramer [26]):

$$T_n = \frac{4 \cdot H}{V_{S\,avg}} = \frac{4}{V_{S\,avg}} \cdot \sum_i h_i \qquad (2)$$

The computed values of Tn for the 13 SMS sites are listed in Table 3 in the column labelled "Tn - $4H/V_{Savg}$" However, as noted above, the shear wave velocity profiles for the SMS sites only extended down to bedrock for three of the 13 stations (i.e., CMHS, HVSC and LPCC). For these three cases, the listed Tn values are for the entire soil column (i.e., the layers above bedrock). However, for the remaining 10 SMS sites, the depth to bedrock is unknown and the listed Tn values are for a soil column that extends only to the maximum depth of the Vs profile. As a result, the listed Tn values are lower-bound estimates of the fundamental period of the soil column (i.e., the greater the depth to bedrock, the longer the natural period).

The second approach used to estimate Tn for the SMS sites assumed that the profile is visco-elastic, with each layer having a damping ratio of 5%. Assuming that the layers behaved as Kelvin-Voigt solids, consistent with the visco-elastic assumption, the small strain transfer functions from bedrock (or the maximum depth of the Vs profile) were computed for each SMS site. The fundamental period of the profile corresponds to the maximum peak in the transfer function (e.g., Kramer [26]). Figure 4a shows the computed transfer function for the CBGS site, which has a Tn = 0.581 s. The Tn values for the other SMS sites are listed in Table 3 in the column labelled "Tn – Trans Func" As with the first approach to estimate Tn, the values determined from the transfer functions are lower bound estimates of the fundamental period for those 10 sites where the Vs profile did not extend to bedrock.

The final approach to estimate Tn for the SMS sites used the ratios of the horizontal to vertical Fourier amplitude spectra (FAS) of the surface motions recorded at the respective stations (i.e., H/V spectral ratios). The premise of the H/V spectral ratio approach is that the vertical component of ground surface motions reflects only source and path effects and is not significantly influenced by site effects. In contrast, the horizontal component of ground surface motions reflects source, path, and site effects. As a result, the H/V spectral ratios primarily reflect site effects, similar to the transfer function, and the source and path effects largely normalize out [27].

Table 3: Supplemental information for strong motion stations (SMS) in, and around, Christchurch, New Zealand

Station Code	Vs30 (m/s)	Tn - $4H/V_{Savg}$ (sec)	Tn - Trans Func (sec)	Tn - H/V (sec)	Original Assumed Seismic Site Class	Updated Seismic Site Class
CBGS	187	> 0.72	> 0.58	0.45	D	E*
CCCC	198	> 0.88	> 0.63	0.71	D	E
CHHC	194	> 0.69	> 0.60	0.53	D	E**
CMHS	204	0.55	0.54	0.72	D	E**
HPSC	206	> 0.62	> 0.44	0.45	E	D/E***
HVSC	422	0.22	0.19	0.42	C	C
KPOC	255	> 0.72	> 0.52	0.36	E	D/E***
LPCC	792	0.09	0.08	0.16	B	C
NNBS	211	> 0.64	> 0.47	0.73	E	E
PRPC	206	> 0.63	> 0.53	0.83	E	E*
REHS	141	> 0.86	> 0.70	0.65	D	E
RHSC	293	> 0.57	> 0.44	0.35	D	C/D****
SHLC	207	>0.68	> 0.52	0.54	D/E	D

* Profile with +10 m of Vs < 165 m/s (i.e., Vs within +10% of 150 m/s Site Class E boundary). Refer to text for more details.

** Profile with +20 m of Vs < 180 m/s (i.e., Vs within +20% of 150 m/s Site Class E boundary). Refer to text for more details.

*** Dual classification (D/E) assigned since profile contains +8 m of Vs < 150 m/s (slightly thinner than than the 10 m criteria for E).

**** Natural period estimates vary sufficiently that a dual classification (C/D) has been assigned.

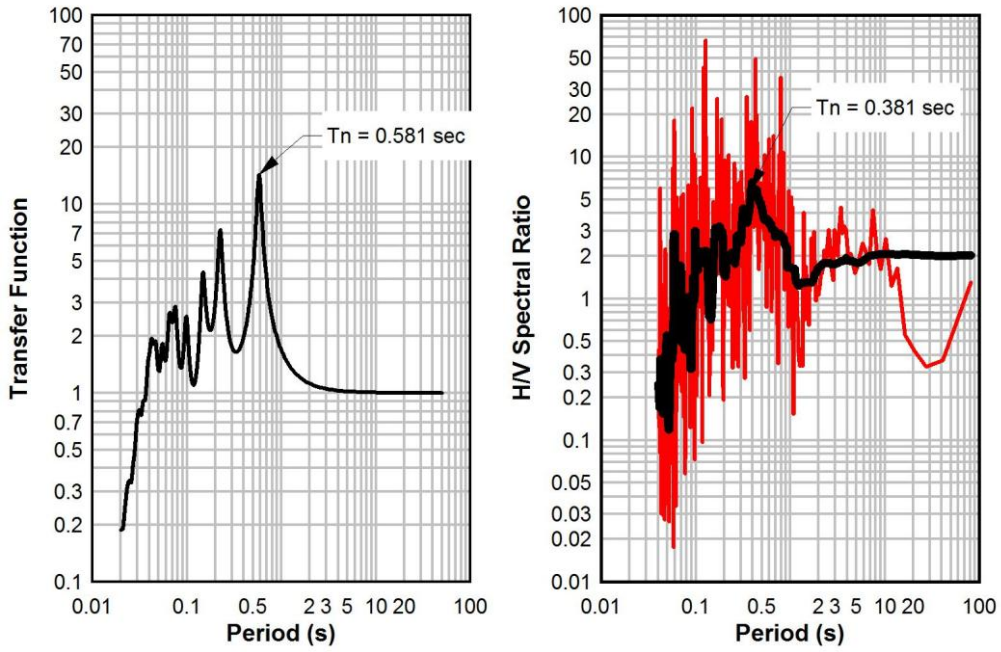

(a) (b)

Figure 4: ***Transfer function (a) and H/V spectral ratio (Red: calculated with no smoothing function applied; Black: smoothing function applied) for a single event; (b) for station CBGS.***

In lieu of using recordings of ambient noise to compute H/V spectral ratios, as originally proposed by Nakamura [27], we used recorded earthquake motions, similar to studies by Lermo and Chavez-Garcia [28], Field and Jacob [29] and Bessason and Kaynia [30]. The earthquake motions were from nine events that occurred between 4 September 2010 and 13 June 2011 and ranged in magnitude from M_w4.7 to M_w7.1. The epicentral locations for these events are shown in Figure 1. Not all stations recorded all nine events, but all the stations recorded at least six of them. Figure 4b shows the computed H/V spectral ratio for the N89W component of motion recorded at CBGS during the M_w5.0, 16 April 2011 earthquake. As shown in this figure, the peaks in the computed spectral ratios vary significantly from one period to the next. Consequently, all the spectral ratios were smoothed by applying a running median function. The sizes of the smoothing windows were increased until the two horizontal components of motion recorded during a given event for a given SMS showed similar trends. The period corresponding to the maximum peak in the smoothed H/V spectral ratio was designated as Tn.

As stated previously, all of the SMS recorded motions from at least six of the nine events considered. Consequently, each station had multiple Tn values, which for a few sites ranged widely. The range in Tn values for a given site is a function of both the limitations of the H/V spectral ratio approach and the varying intensity of the ground shaking that the sites experience in the nine events. As opposed to the two approaches outline above that used small strain Vs profiles to estimate Tn, the strains inherent to the H/V spectral ratio approach used herein were in some cases very large. However, so as to not be significantly influenced by outliers, the median Tn values for each of the stations were used and are listed in Table 3 in the column labelled "Tn – H/V".

Of the Tn values listed in Table 3, we recommend the values determined using the transfer function approach. This is because a transfer function accurately reflects the dynamic response characteristics of the layered profiles and little to no judgement was required to determine the Tn values once the transfer functions were computed. Second preference is given to the equivalent uniform profile approach (i.e., the $4H/V_{Savg}$ approach). The transfer function and the equivalent uniform profile approaches yield similar results for simple soil profiles (e.g., uniform profiles or profiles that monotonically increase in stiffness with depth), especially when a strong bedrock contrast exists in the resolvable depth (i.e., note the close agreement in Tn for these two methods at CMHS, HVSC and LPCC). However, when the two approaches yield significantly different results, it reflects the shortcoming of modelling a complex layered system as a single, uniform layer rather than reflecting any shortcoming in the transfer function methodology. Caution should be particularly exercised in using the $4H/V_{Savg}$ approach to compute Tn for profiles having soft layers sandwiched between stiffer layers. Finally, the H/V spectral ratio approach is given last preference for estimating Tn. This approach requires considerable judgement regarding both selecting the motions used, windowing of the selected motions, and determining Tn from the smoothed ratios. As a result, this approach is not recommended for the casual user.

SEISMIC SITE CLASSIFICATION

The New Zealand Loadings Standard (NZS1170.5) [14] uses a simplified seismic site classification system, similar to other international standards such as Eurocode 8 (EC8) [31] or the International Building Code (IBC) [32]. These systems use five or six general soil classifications that are established by the stiffness and layering at a site. Similar to other codes, each building site in a seismic area must be designated as Site Class A-E; where A is strong rock, B is rock, C is shallow soil, D is deep or soft soil, and E is very soft soil. The NZS1170.5 system differs slightly in how these seismic sites classes are determined as compared to EC8 and IBC. Site class per EC8 and IBC are almost exclusively defined based on Vs30 values, whereas NSZ1170.5 uses Vs30 in combination with the Tn of a site to obtain the seismic classification. Tn has been shown to provide a better estimate of amplification than Vs30 at sites

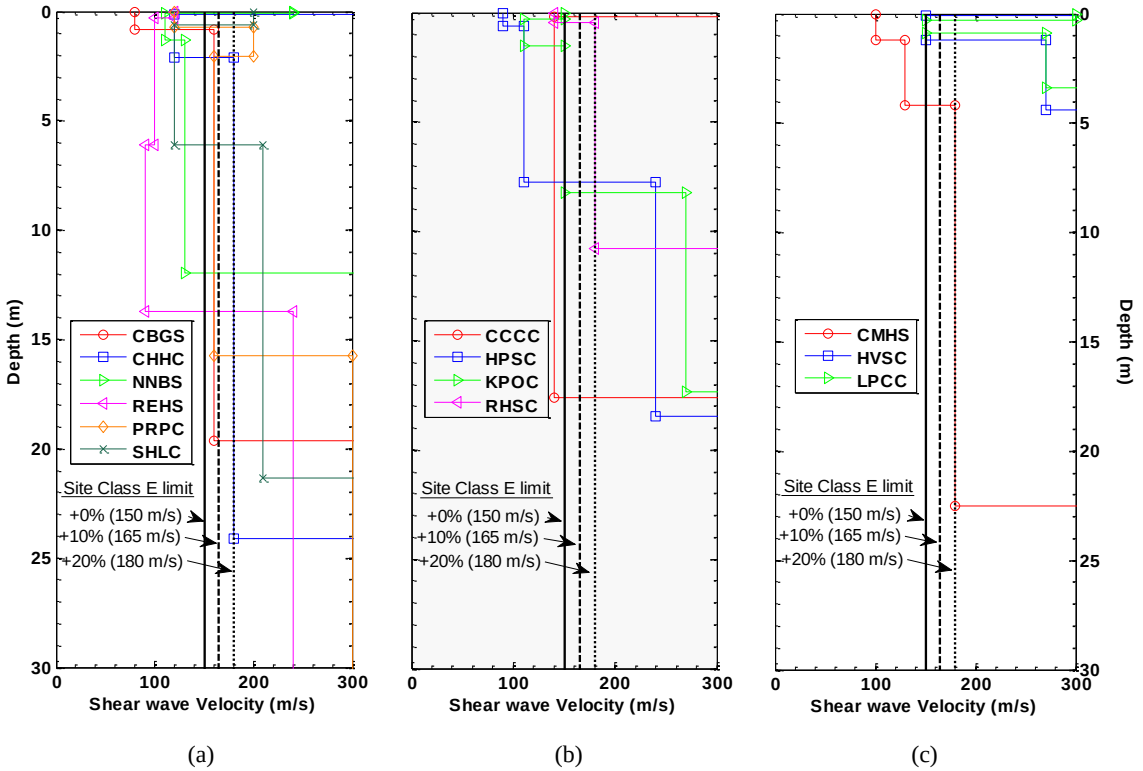

Figure 5: ***Vs profiles with (a) V_{smax} < 400 m/s with Site Class E limit); (b) Vs profiles with 400 <V_{smax}< 600 with Site Class E limit and (c) Vs profiles with V_{smax}> 600 m/s with Site Class E limit.***

where a thick layer of soft soil extends beyond 30 m below the surface. In NSZ1170.5, a major division in site classification occurs at Tn = 0.6 s, which is the threshold between Site Classes C and D. An increase of 63% in the design response spectra exists between those site classes [33]. As a result, sites with borderline natural periods can have very different seismic design requirements depending on their site class.

Both the currently assumed seismic site classifications and the revised/updated classifications for the 13 SMS characterized in the present work are provided in Table 3. Some of the sites were easy to classify and others required some interpretation/engineering judgement. The Vs profiles were relied on heavily, not just for Vs30 calculations and Tn estimates, but also for layering that might indicate Site Class E soils (i.e., soils +10 m thick with Vs < 150 m/s). As discussed in the Site Period Estimates section, preference was given to Tn estimated from the transfer function approach. However, the other values of Tn were considered, at least partially, when assigning site class. Three sites (HPSC, KPOC, and RHSC) received dual classifications due to the complexity of the information, and a number of Site Class E sites required interpretation beyond the criteria outlined in NSZ1170.5 [14].

Figure 5 is a zoomed in view of the Vs profiles presented in Figure 3. This figure was used to aid in determining profiles that may be designated as Site Class E. The Site Class E Vs boundary of 150 m/s is designated on each of the three subplots. Also designated is a 165 m/s and a 180 m/s boundary, which correspond to +10% and +20% of the 150 m/s boundary, respectively. As per Section 3.1.3.6 of NZS1170.5, any SMS site with +10 m of soil with Vs < 150 m/s was classified as Site Class E. Additionally, any SMS site with +10 m of Vs < 165 m/s soil was classified as Site Class E. This is outside the strict boundaries of Section 3.1.3.6, but Vs estimates from surface wave methods are generally only considered accurate within 10%. Therefore, the +10% boundary in Figure 5 was used to determine any Vs profiles that had +10 m of soil that met this criteria and they were also designated as Site Class E. These SMS sites have a single * next to the classification in Table 3. Two additional sites with Vs ranging up to 180 m/s were also designated as Site Class E. Again, these sites did not meet the strict Site Class E requirements, but instead had Vs profiles that indicated +20 m of soil with Vs < 180 m/s. Therefore, these sites (indicated by a two ** in Table 3) were designated as Site Class E due to soil layers that exceeded the thickness criteria of Section 3.1.3.6 by at least two times, but fell outside of the 150 m/s Vs boundary by less than 20%.

Two SMS sites were designated as borderline Site Class D/E (i.e, HPSC and KPOC). We feel that these sites are more closely aligned with Site Class E, but could not justify that designation as clearly as for the sites discussed above. Both sites are underlain by approximately 8 m of soil with Vs < 150 m/s, which is 20% thinner than the +10 m criteria in Section 3.1.3.6. However, these sites were close enough to the criteria to justify a dual classification. One SMS site was designated as border line Site Class C/D (i.e, RHSC). We feel that this site is more closely aligned with Site Class D, but could not fully justify that designation based on the available information. The boundary between Site Class B and D is primarily based on a limiting Tn of 0.6 s (i.e., sites with Tn > 0.6 s that do not classify as Site Class A, B or E are designated Site Class D, while sites with Tn < 0.6 s are designated Site Class C). However, the Tn estimates (refer to Table 3) from the methods discussed above were sufficiently scattered (ranging from > 0.57 s to > 0.44 s for the two most trusted methods) to make this designation uncertain. Additionally, the Vs profile for RHSC indicated +10 m of soil with Vs < 180 m/s (just outside the Site Class E category). Therefore, RHSC was designated as dual Site Class C/D.

SMS LPCC was originally assumed as Site Class B. Indeed, the Vs30 value based on the measured Vs profile is 792 m/s, which is greater than the 760 m/s boundary in Section 3.1.3.3.

However, the Vs profile also indicates +3 m of material with Vs < 300 m/s, which excludes it from Site Class B. Therefore, LPCC was designated as Site Class C based on Tn. Additionally, the Vs testing location is approximately 300 m from the SMS location. Therefore, the SMS profile could be located on material differing from that presented herein. Classification of the SMS sites not specifically discussed above was fairly straight forward

CONCLUSIONS

This paper details efforts to characterize the small-strain dynamic properties of 13 SMS sites in the greater Christchurch, New Zealand area. Little information about the subsurface layering and dynamic characteristics at these 13 SMS was available prior to our work. We performed active- and passive-source surface wave testing to obtain shear wave velocity (Vs) profiles at each site. The Vs profiles were used to calculate the average Vs over the top 30 m of the subsurface and to estimate the natural period of vibration (Tn). Additionally, estimates of Tn were obtained by computing the horizontal-to-vertical spectral ratios from recorded GM at each SMS. Based on this new information, we have updated the site classifications at the 13 SMS sites tested; 10 of which ended up with a slightly different site classification than the original assumption (often one site class lower).

Challenges involved in designating seismic site classification at several SMS sites reinforce the difficulties that can be encountered in grouping all possible site conditions into one of five generalized categories. The impact of this work is greater than simply updating seismic site classifications at these SMS sites. The Vs profiles and Tn estimates provided herein will allow for more detailed site-specific studies that will help piece together the complicated ground response during the Canterbury earthquake sequence. Additional studies are needed to correlate the dynamic properties now available for these sites with the amplitude, frequency content and duration of motions recorded during each event. These studies should lead to better predictive models for levels of ground shaking during future earthquakes.

ACKNOWLEDGEMENTS

The primary support for R. Green, B. Cox, and C. Wood was provided by the U.S. National Science Foundation (NSF) RAPID grant CMMI-1137977. Also, L. Wotherspoon's position at the University of Auckland is funded by the Earthquake Commission (EQC). However, any opinions, findings, and conclusions or recommendations expressed in this material are those of the authors and do not necessarily reflect the views of the National Science Foundation or the EQC. We acknowledge the New Zealand GeoNet project and its sponsors EQC, GNS Science and LINZ, for providing ground motion records used in this study.

REFERENCES

1 Gledhill, K., Ristau, J., Reyners, M., Fry, B. and Holden, C. (2011) "The Darfield (Canterbury, New Zealand) Mw 7.1 earthquake of September 2010: A preliminary seismological report". *Seismological Research Letters*, **82** (3): 378-386.

2 GNS Science (2011) Geonet http://www.geonet.org.nz (accessed September 10, 2011)

3 Avery, H.R., Berrill, J.B., Coursey, P.F., Deam, B.L., Dewe, M.B., Francois, C.C., Pettinga, J.R., and Yetton, M.D. (2004) "The Canterbury University strong-motion recording project". *Proc. 13th World Conference on Earthquake Engineering*, Vancouver, British Columbia, August 1- 6, 2004.

4 Nazarian, S. and Stokoe II, K.H. (1984) "In situ shear wave velocities from spectral analysis of surface wave tests". *Proc. Eighth World Conference on Earthquake Engineering*, San Francisco, California, 31-38.

5 Stokoe, K.H., Wright, S.G., Bay, J.A., and Roesset, J.M. (1994) "Characterization of geotechnical sites by SASW method". *Proc. 13th International Conference on Soil Mechanics and Foundation Engineering*, **22** (9-12). New Delhi, India, 923-930.

6 Park, C.B., Miller, R.D. and Xia, J. (1999) "Multichannel analysis of surface waves". *Geophysics*, **64**: 800-880.

7 Louie, J.N. (2001) "Faster, better shear wave velocity to 100 meters depth from refraction microtremor arrays". *Bulletin of Seismological Society of America*, **91** (2): 347-364.

8 Park, C.B., and Miller, R.D. (2008) "Roadside Passive Multichannel Analysis of Surface Waves (MASW)". *Journal of Env. & Eng. Geophys*, **13** (1): 1-11.

9 Tokimatsu, K., Shinzawa, K., and Kuwayama, S. (1992) "Use of short-period microtremors for Vs profiling". *Journal of Geotechnical Engineering*, **118** (10): 1544-1558.

10 Okada, H. (2003) "The Microtremor Survey Method". *Geophysical Monograph Series no. 12. Society of Exploration Geophysicists*: 135.

11 Brown, L.J. and Weeber, J.H. (1992) *Geology of the Christchurch urban area*. Institute of Geological and Nuclear Sciences, Lower Hutt.

12 Brown, L.J., Beetham, R.D., Paterson, B.R., and Weeber, J.H. (1995). "Geology of Christchurch, New Zealand". *Environmental & Engineering Geoscience*, **1** (4): 427-488.

13 Wotherspoon, L.M., Pender, M.J., Orense, R.P. (2011) "Relationship between observed liquefaction at Kaiapoi following the 2010 Darfield earthquake and former channels of the Waimakariri River". *Engineering Geology*, Available on line 13 November 2011, doi:10.1016/j.enggeo.2011.11.001

14 Standards New Zealand (2004) *NZS1170.5 Earthquake actions*. Wellington, NZ.

15 Cousins, J., and McVerry, G. (2010) "Overview of strong motion data from the Darfield Earthquake". *Bulletin of the New Zealand Society for Earthquake Engineering*, **43** (4): 222-227.

16 Bradley, B.A. and Cubrinovski, M. (2011) "Near-source strong ground motions observed in the 22 February 2011 Christchurch earthquake". *Seismological Research Letters*, (in review).

17 Allen, J., Ashford, S., Bowman, E., Bradley, B., Cox, B., Cubrinovski, M., Green, R., Hutchinson, T., Kavazanjian, E., Orense, R., Pender, M., Quigley, M., and Wotherspoon, L. (2010a) "Geotechnical Reconnaissance of the 2010 Darfield (Canterbury) Earthquake". *Bulletin of the New Zealand Society for Earthquake Engineering*, **43** (4): 243-320.

18 Allen, J., Ashford, S., Bowman, E., Bradley, B., Cox, B., Cubrinovski, M., Green, R., Hutchinson, T., Kavazanjian, E., Orense, R., Pender, M., Quigley, M. and Wotherspoon, L. (2010b) "Geotechnical Reconnaissance of the 2010 Darfield (New Zealand) Earthquake". (R.A. Green and M. Cubrinovski, eds.), *GEER Association Report No. GEER-024*.

19 Fry, B., Benites, R., Reyners, M., Holden, C., Kaiser, A., Bannister, S., Gerstenberger, M., Williams, C., Ristau, J., Beavan, J. (2011) "Extremely strong shaking in the New Zealand earthquakes of 2010 and 2011". *Eos Transactions, American Geophysical Union*, (submitted).

20 Yoon, S. and Rix, G.J. (2009) "Near-field effects on array-based surface wave methods with active sources". *Journal of Geotechnical and Geoenvironmental Eng.*., **135** (3): 399-406.

21 Cox, B.R. and Beekman, A.N., (2011) "Intramethod Variability in ReMi Dispersion Measurements and Vs Estimates at Shallow Bedrock Sites". *Journal of Geotechnical and Geoenvironmental Eng.*, **137** (4): 354-362.

22 Zywicki, D.J. (1999) "Advanced signal processing methods applied to engineering analysis of seismic surface waves". *Ph.D. Dissertation*, School of Civil and Environmental Engineering, Georgia Institute of Technology, Atlanta, GA, 357 p.

23 Optim (2006) "User's Manual: SeisOpt® ReMi™ Version 4.0." Optim, Inc., Reno, NV. 85p.

24 Cox, B. and Wood, C. (2011) "Surface Wave Benchmarking Exercise: Methodologies, Results and Uncertainties". *Proc. GeoRisk 2011*, Atlanta, GA, June 26-28.

25 Joh, S.H. (1996) "Advances in interpretation and analysis techniques for spectral-analysis-of-surface-waves (SASW) measurements". *Ph.D. Dissertation*, Dept. of Civil, Architectural, and Environmental Engineering, University of Texas, Austin, TX, 240 p.

26 Kramer, S.L. (1996) *Geotechnical Earthquake Engineering*, Prentice Hall, Upper Saddle River, NJ, USA.

27 Nakamura, Y. (1989) "A Method for Dynamic Characteristics Estimation of Subsurface Using Microtremor on the Ground Surface". *Quarterly Report of the Railway Technical Research Institute*, **30** (1): 25-33.

28 Lermo, J. and Chavez-Garcia, F.J. (1993) "Site Effect Evaluation Using Spectral Ratios with Only One Station". *Bulletin of the Seismological Society of America*, **83** (5): 1574–1594.

29 Field, E.H. and Jacob, K.H. (1995) "A Comparison and Test of Various Site-Response Estimation Techniques, Including Three that Are Not Reference-Site Dependent". *Bulletin of the Seismological Society of America*, **85** (4): 1127-1143.

30 Bessason, B. and Kaynia, A.M. (2002) "Site Amplification in Lava Rock on Soft Sediments". *Soil Dynamics and Earthquake Engineering*, **22** (7): 525-540.

31 CEN (2004) *EN 1998-1 Eurocode 8: Design of structures for earthquake resistance*, Brussels, Belgium.

32 International Code Council, Inc. (ICC) (2009) *International Building Code*, Washington DC.

33 McVerry, G. (2011) "Site-effect terms as continuous functions of site period and Vs30". *Proc. Ninth Pacific Conference on Earthquake Engineering*, Auckland, New Zealand, April 14-16.